Eur. Phys. J. C 52, 305–314 (2007)
DOI 10.1140/epjc/s10052-007-0394-4

THE EUROPEAN PHYSICAL JOURNAL C

Regular Article – Theoretical Physics

Hadron masses in QCD with one quark flavour

F. Farchioni[1], I. Montvay[2,a], G. Münster[1], E.E. Scholz[3], T. Sudmann[1], J. Wuilloud[1]

[1] Universität Münster, Institut für Theoretische Physik, Wilhelm-Klemm-Strasse 9, 48149 Münster, Germany
[2] Deutsches Elektronen-Synchrotron DESY, Notkestr. 85, 22603 Hamburg, Germany
[3] Physics Department, Brookhaven National Laboratory, Upton, NY 11973, USA

Received: 9 July 2007 /
Published online: 6 September 2007 –

Abstract. One-flavour QCD – a gauge theory with SU(3) colour gauge group and a fermion in the fundamental representation – is studied by Monte Carlo simulations. The mass spectrum of the hadronic bound states is investigated in a volume with extensions of $L \simeq 4.4r_0$ ($\simeq 2.2$ fm) at two different lattice spacings: $a \simeq 0.37r_0$ ($\simeq 0.19$ fm) and $a \simeq 0.27r_0$ ($\simeq 0.13$ fm). The lattice action is a Symanzik tree-level improved Wilson action for the gauge field and an (unimproved) Wilson action for the fermion.

1 Introduction

QCD with one flavour of quarks is an interesting theoretical laboratory to study some aspects of the strong interaction dynamics, namely those not connected to spontaneous chiral symmetry breaking and to the existence of light pseudo-Goldstone bosons. As a consequence of a quantum anomaly, the U(1) axial symmetry of the classical Lagrangian is broken and in the limit of vanishing quark mass no massless Goldstone boson exists.

An intriguing possibility at negative quark masses is the spontaneous breakdown of parity and charge conjugation symmetry – a phenomenon first conjectured by Dashen [1] in the three-flavour theory. This has to do with the possible negative sign of the fermion determinant at negative quark masses, because under the assumption of the positiveness of the fermion determinant Vafa and Witten [2] proved the impossibility of this kind of spontaneous symmetry breaking.

A dramatic consequence of the absence of (broken) chiral symmetry is the difficulty to find a unique definition of the point with zero quark mass in parameter space [3–5]. (For an excellent summary and discussion of this problem see [6].)

Another line of recent theoretical developments is the relation between one-flavour ($N_f = 1$) QCD and supersymmetric Yang–Mills (SYM) theory with one supersymmetry charge ($\mathcal{N} = 1$) [7–10]. This connection is the consequence of *orientifold planar equivalence* in the limit of large number of colours ($N_c \to \infty$). This might imply approximate relations among hadron masses even at $N_c = 3$, for instance, the approximate degeneracy of scalar and pseudoscalar bound states of quarks [11] reflecting the properties of the Veneziano–Yankielovicz low-energy effective action of $\mathcal{N} = 1$ SYM [12] in the mass spectrum of $N_f = 1$ QCD. For instance, the ratio of the mass of the lowest pseudoscalar meson to the mass of the scalar meson is predicted, including $1/N_c$ corrections, to be $(N_c - 2)/N_c$ [13, 14]. Another prediction of orientifold equivalence is the size of the quark condensate in one-flavour QCD, which has recently been compared with numerical simulation results in [15].

In the present paper we start to explore the mass spectrum of hadronic states in one-flavour QCD by numerical Monte Carlo simulations. This requires reasonably large physical volumes at small quark masses and high statistics – especially for determining glueball masses and contributions of disconnected quark diagrams. We apply the Wilson lattice fermion action, which has recently been shown by several collaborations [16–20] to be well suited for such an investigation. We start our exploratory studies here on $12^3 \cdot 24$ and $16^3 \cdot 32$ lattices with lattice spacing $a \simeq 0.19$ fm and $a \simeq 0.13$ fm, respectively. This means that our present setup roughly corresponds to the earlier simulations of the qq+q Collaboration [16, 17], but we hope to continue these investigations in the near future closer to the continuum limit as in [18–20].

For setting the scale we use the Sommer parameter [21] r_0, which we set by definition to be $r_0 \equiv 0.5$ fm. In other words, whenever we speak about "1 fm" we always mean "$2r_0$" – having in mind that one-flavour QCD is a theory different from QCD realised in nature.

Since the sign of the quark determinant is a sensitive issue, we carefully determine it and take it into account in determining the expectation values. In the present paper we choose the quark mass to be sufficiently far away from zero on the positive side, where the effect of the determinant sign is not very strong. In spite of this, as we shall see, we can investigate quite small quark masses down to $m_q \simeq 12$ MeV (that is $m_q r_0 \simeq 0.03$), corresponding to a pion mass $m_\pi \simeq 270$ MeV.

[a] e-mail: montvay@mail.desy.de, istvan.montvay@desy.de

Let us mention that keeping the quarks sufficiently heavy (choosing the hopping parameter κ in the Wilson fermion action (2) below $\frac{1}{8}$) the problem of negative quark determinants can be avoided. (The thermodynamics of $N_f = 1$ QCD for heavy quarks has been investigated under this assumption in [22].) Our aim is, however, to reach small quark masses and therefore we have to deal with the possibly negative sign of the quark determinant.

For interpreting our results on the mass spectrum we find it useful to embed the $N_f = 1$ QCD theory in a *partially quenched* theory with more quark flavours. This embedding is particularly useful if the additional quenched *valence* quark flavours have the same mass as the dynamical *sea* quark because of the exact SU(N_F) flavour symmetry in the combined sea- and valence-sectors (N_F denotes here the total number of quenched and unquenched flavours). In most cases we consider the natural choice $N_F = 3$, which is closest to the situation realised in nature. We also work out some of the predictions of *partially quenched chiral perturbation theory* (PQChPT) and compare them to the numerical data.

The plan of this paper is as follows: in the next section we define the lattice action and briefly discuss the updating algorithm. In Sect. 3 the partially quenched viewpoint is introduced and PQChPT is considered for it. Section 4 is devoted to the presentation of our numerical simulation data. The last section contains a discussion and summary.

2 Lattice action and simulation algorithm

2.1 Lattice action

For the SU(3) Yang–Mills gauge field we apply, following [20], the *tree-level improved Symanzik* (tlSym) action, which is a generalisation of the Wilson plaquette gauge action. It belongs to a one-parameter family of actions obtained by renormalisation group considerations in the Symanzik improvement scheme [23]. Those actions also include, besides the usual (1×1) Wilson loop plaquette term, planar rectangular (1×2) Wilson loops:

$$S_g = \beta \sum_x \left(c_0 \sum_{\mu<\nu,\,\mu,\nu=1}^{4} \left\{ 1 - \frac{1}{3}\mathrm{Re} U^{1\times 1}_{x\mu\nu} \right\} + c_1 \sum_{\mu\neq\nu,\mu,\nu=1}^{4} \left\{ 1 - \frac{1}{3}\mathrm{Re} U^{1\times 2}_{x\mu\nu} \right\} \right) , \tag{1}$$

with the normalisation condition $c_0 = 1 - 8c_1$. For the tlSym action we have $c_1 = -1/12$ [24–26].

The fermionic part of the lattice action is the simple (unimproved) Wilson action:

$$S_f = \sum_x \left\{ \overline{\psi}^a_x \psi^a_x - \kappa \sum_{\mu=1}^{4} \left[\overline{\psi}^a_{x+\hat{\mu}}\, U_{ab,x\mu} (1+\gamma_\mu) \psi^b_x + \overline{\psi}^a_x\, U^\dagger_{ab,x\mu} (1-\gamma_\mu) \psi^b_{x+\hat{\mu}} \right] \right\} . \tag{2}$$

Here κ is the hopping parameter related to the bare quark mass in lattice units am_0 by

$$\frac{1}{2\kappa} = am_0 + 4 . \tag{3}$$

The Wilson parameter removing the fermion doublers in the continuum limit is fixed in (2)–(3) to $r = 1$.

2.2 Simulation algorithm

For preparing the sequences of gauge configurations a *Polynomial Hybrid Monte Carlo* (PHMC) updating algorithm was used, which is well suited for theories with an odd number of fermion species. This algorithm is based on multi-step (actually two-step) polynomial approximations of the inverse fermion matrix with stochastic correction in the update chain as described in [27, 28]. The starting point is the PHMC algorithm as introduced in [29–32]. The polynomial approximation scheme and the stochastic correction in the update chain are taken over from the two-step multi-boson algorithm of [33]. For details of the updating algorithm and for notation related to it see [27, 28].

In order to speed up the updating, *even–odd preconditioning* was used, which pushes the small eigenvalues of the (squared Hermitean) fermion matrix $Q[U]^2$ to larger values. The eigenvalues of $Q[U]^2$ are assumed to be covered on typical gauge configurations by the approximation interval $[\epsilon, \lambda]$. In exceptional cases some of the eigenvalues (typically just the smallest one) are outside this interval. In order to correct for this a *correction factor* $C[U]$ is associated with such configurations. The exact value of this correction factor can be written as

$$C[U] = \left\{ \prod_i \left[\lambda_i^{1/(2n_B)} P_1(\lambda_i) P_2(\lambda_i) \right] \right\}^{n_B} . \tag{4}$$

Here the product runs over the eigenvalues of $Q[U]^2$, the polynomial $P_1(x)$ is an approximation for $x^{-1/(2n_B)}$, $P_2(x)$ for $[x^{1/(2n_B)} P_1(x)]^{-1}$. The positive integer n_B defines the *determinant break-up* which means that in the path integral the fermions are represented by

$$\left[\left(\det Q[U]^2 \right)^{1/(2n_B)} \right]^{n_B} . \tag{5}$$

The part of the product in (4) where λ_i is inside the interval $[\epsilon, \lambda]$ can be effectively replaced by a stochastic estimator and then

$$C[U] = \left\{ \prod_j{}' \left[\lambda_j^{1/(2n_B)} P_1(\lambda_j) P_2(\lambda_j) \right] \times \frac{1}{N'} \sum_{n=1}^{N'} \exp\left[\eta_n^\dagger \Big(1 - P'(Q[U]^2) \Big) \eta_n \right] \right\}^{n_B} . \tag{6}$$

Here the $\prod'_j$ runs over the eigenvalues outside the interval $[\epsilon, \lambda]$, $P'(x)$ is a sufficiently good approximation

of $[x^{1/(2n_B)}P_1(x)P_2(x)]^{-1}$, N' is the arbitrary number of stochastic estimators and the η_n are Gaussian vectors in the subspace orthogonal to the eigenvectors corresponding to the eigenvalues λ_j. In practice, one can choose the polynomial $P_2(x)$ to be such a good approximation that the stochastic part in (6) has no noticeable effect on the expectation values and therefore can completely be neglected. In this case the correction factor is simply given by

$$C[U] = \left\{ \prod_j{}' \left[\lambda_j^{1/(2n_B)} P_1(\lambda_j) P_2(\lambda_j) \right] \right\}^{n_B} . \qquad (7)$$

Besides the correction factor $C[U]$, the sign $\sigma[U]$ of the fermion determinant $\det Q[U]$ has also to be included in the *reweighting* of the configurations and then the expectation value of a quantity A is given by

$$\langle A \rangle = \frac{\int \mathrm{d}[U]\sigma[U]C[U]A[U]}{\int \mathrm{d}[U]\sigma[U]C[U]} . \qquad (8)$$

This formula shows the dangerous *sign problem*, which can arise due to the fluctuation of the determinant sign because in case of strong fluctuations of $\sigma[U]$ both nominator and denominator on the right hand side may become small, spoiling the statistical accuracy. (Similarly, one can also lose statistics if the correction factors $C[U]$ are much smaller than 1 on many configurations.)

Typical values of the approximation interval and of the polynomial orders at the lightest quark mass simulated on $12^3 \cdot 24$ and $16^3 \cdot 32$ lattices, respectively, are collected in Table 1. As in [27, 28], the orders of the polynomials P_j, $(j = 1, 2)$ are denoted by n_j and those of $\bar{P}_j$, $(j = 1, 2)$ by $\bar{n}_j$, respectively. The simulations have been done with determinant break-up $n_B = 2$. (The polynomials $\bar{P}_j$ are approximating $(P_j)^{-\frac{1}{2}}$. For more details see [27, 28] and references therein.)

The last four columns of Table 1 show the values of the *deviation norm* δ, which is minimised for a given polynomial order n in the *least-square approximation* scheme we are using. Generically δ is defined as

$$\delta \equiv \left\{ \frac{\int_\epsilon^\lambda \mathrm{d}x w(x) \Big[f(x) - P_n(x) \Big]^2}{\int_\epsilon^\lambda \mathrm{d}x w(x) f(x)^2} \right\}^{\frac{1}{2}} . \qquad (9)$$

Here $f(x)$ is the function to be approximated and $w(x)$ is a positive weight function actually chosen in our case to be $w_1(x) = w_2(x) = x^{1/(2n_B)}$ and $\bar{w}_1(x) = \bar{w}_2(x) = 1$, respectively. The values of δ_1 in Table 1 are such that the average acceptance rate of the stochastic correction at the end of trajectory sequences is between 80%–90%. The other δ values are small enough to ensure practically infinite precision of the expectation values. For more details on the algorithmic setup in our runs see also Sect. 4.

3 Partially quenched viewpoint

Because the classical $\mathrm{U(1)_A}$ axial symmetry is anomalous, the single-flavour QCD theory does not have a continuous chiral symmetry apart from the U(1) quark number symmetry. Consequently it does not have spontaneous chiral symmetry breaking and hence no (pseudo-) Goldstone bosons and no easy definition of the quark mass [3–5]. In the lattice regularisation it is, however, possible to enhance the symmetry artificially by adding extra *valence quarks*, which are *quenched*, that is, are not taken into account in the Boltzmann weight of the gauge configurations by their fermion determinants. In principle, one might consider any number of quenched valence quarks with any mass values but, to remain close to QCD realised in nature, the most natural choice is to take two equal-mass valence quarks and to call them u and d quarks. The original dynamical quark can then be called s quark where "s" may stand for *sea* or *strange*. The theory with dynamical s quark and quenched u and d quarks is *partially quenched*. (Observe that this partially quenching is somewhat unconventional, since some of the valence quarks are quenched but taken degenerate with the sea quark.)

Using this terminology, for instance, the pseudoscalar bound state of s and $\bar{s}$ can be called η_s. The corresponding scalar state is then σ_s. The lowest baryon state consisting of s quarks, which has to have spin $\frac{3}{2}$ because of the Pauli principle, can be named Ω^- or e.g. Δ_s etc.

A theoretical description of partially quenched QCD can be obtained through the introduction of ghost quarks [36]. For each (quenched) valence quark a corresponding bosonic ghost quark is added to the model. The functional integral over the ghost quark fields then cancels the fermion determinant of the valence quarks and only the sea quark determinant remains in the measure. In our case there are 2 flavours of valence quarks and ghost quarks, each, with equal masses m_{V}, and a single flavour of sea quarks with mass m_{S}.

A particularly interesting point of the partially quenched theory is the one where all the three quark masses are equal. In this point there is an exact SU(3) vector-like flavour symmetry in the valence plus sea quark sector, and the hadronic bound states appear in exactly degenerate

Table 1. Algorithmic parameters in the runs with lightest quark mass on $12^3 \cdot 24$ (first line) and $16^3 \cdot 32$ (second line) lattice, respectively. For notation see the text and also [27, 28]

ϵ	λ	n_1	$\bar{n}_1$	n_2	$\bar{n}_2$	δ_1	$\bar{\delta}_1$	δ_2	$\bar{\delta}_2$
3.25×10^{-6}	2.6	350	550	1400	1600	4.9×10^{-4}	6.7×10^{-7}	9.9×10^{-7}	8.8×10^{-7}
1.20×10^{-5}	2.4	250	370	1000	1150	5.4×10^{-4}	8.2×10^{-7}	4.8×10^{-7}	3.1×10^{-7}

SU(3)-symmetric multiplets. For instance, there is a degenerate octet of pseudoscalar mesons – the "pions" (π^a, $a = 1, \ldots, 8$) satisfying an SU(3)-symmetric PCAC relation. With the help of the divergence of the axialvector current $A^a_{x\mu}$ and pseudoscalar density P^a_x one can define, as usual, the bare *PCAC quark mass* $am_{\rm PCAC}$ in lattice units:

$$am_{\rm PCAC} \equiv \frac{\langle \partial^*_\mu A^+_{x\mu} P^-_y \rangle}{2\langle P^+_x P^-_y \rangle} \,. \tag{10}$$

Here the indices + and − refer to the "charged" components corresponding to $\lambda_a \pm \mathrm{i}\lambda_b$ (with $\lambda_{a,b}$ some off-diagonal Gell-Mann matrices) and ∂^*_μ denotes the backward lattice derivative. Due to the exact SU(3) symmetry, the renormalised quark mass corresponding to $m_{\rm PCAC}$ can be defined by an SU(3)-symmetric multiplicative renormalisation:

$$m^{\rm R}_{\rm PCAC} = \frac{Z_{\rm A}}{Z_{\rm P}} m_{\rm PCAC} \,. \tag{11}$$

By tuning the bare quark mass on the lattice suitably, the masses of the "pions" can be made to vanish, as the numerical results indicate, and the renormalised quark mass vanishes, too. At this point the partially quenched theory has a graded $\mathrm{SU}(N_F|N_{\rm V})_{\rm L} \otimes \mathrm{SU}(N_F|N_{\rm V})_{\rm R}$ symmetry, which is broken spontaneously to a "flavour" $\mathrm{SU}(N_F|N_{\rm V})$. (Here $N_{\rm V}$ is the number of additional valence quark flavours and $N_F \equiv N_{\rm V} + N_f = N_{\rm V} + 1$.) In our case, with $N_{\rm V} = 2$ flavours of valence quarks, the symmetry is thus SU(3|2). The "pions" are the Goldstone bosons of the broken SU(3) subgroup.

Adding generic quark masses $m_{\rm V}$ and $m_{\rm S}$, the symmetry group is explicitly broken down to SU(2|2). In the special case $m_{\rm V} = m_{\rm S}$, considered here, the symmetry is still SU(3|2), and its subgroup SU(3) is the flavour symmetry mentioned above.

The "pions" are, of course, not physical particles in the spectrum of $N_f = 1$ QCD. Nevertheless, their properties such as masses and decay constants are well defined quantities, which can be computed on the lattice. The same is true of the PCAC quark mass $m^{\rm R}_{\rm PCAC}$, which is therefore a potential candidate for a definition of a quark mass of this theory.

The relation between the pion masses and the quark masses can be considered in partially quenched chiral perturbation theory [37–39], including effects of the lattice spacing a [40–44]. The pseudo-Goldstone fields are parameterized by a graded matrix,

$$U(x) = \exp\left(\frac{\mathrm{i}}{F_0}\Phi(x)\right) \tag{12}$$

in the supergroup SU(3|2). (Here the normalization of F_0 is such that its phenomenological value is $\simeq 86$ MeV.) The commuting elements of the graded matrix Φ represent the pseudo-Goldstone bosons made from a quark and an antiquark with equal statistics, and the anticommuting elements of Φ represent pseudo-Goldstone fermions that are built from one fermionic quark and one bosonic quark. The supertrace of Φ has to vanish, which can be implemented by a suitable choice of generators [45].

We have calculated the masses of the pseudo-Goldstone bosons in next-to-leading order of partially quenched chiral perturbation theory along the lines of [45], including $O(a)$ lattice effects [42]. The quark masses enter the expressions in the combinations

$$\chi_{\rm V} = 2B_0 m_{\rm V}, \quad \chi_{\rm S} = 2B_0 m_{\rm S} \,, \tag{13}$$

with the usual low-energy constant B_0, and the lattice spacing occurs as

$$\rho = 2W_0 a \,, \tag{14}$$

where W_0 is another, lattice-specific, low-energy constant. For the pion masses we obtain

$$\begin{aligned} m^2_{\rm VV} \equiv m^2_\pi = {} & \chi_{\rm V} + \rho + \frac{\chi_{\rm V}+\rho}{16\pi^2 F_0^2}\Big[\chi_{\rm V} - \chi_{\rm S} \\ & + (2\chi_{\rm V} - \chi_{\rm S} + \rho)\ln\left(\frac{\chi_{\rm V}+\rho}{16\pi^2 F_0^2}\right)\Big] \\ & + \frac{8}{F_0^2}\left[(2L_8 - L_5)\chi_{\rm V}^2 + (2L_6 - L_4)\chi_{\rm V}\chi_{\rm S}\right. \\ & + (2W_8 + W_6 - W_5 - W_4 - L_5)\rho\chi_{\rm V} \\ & \left. + (W_6 - L_4)\rho\chi_{\rm S}\right] , \end{aligned} \tag{15}$$

where the usual low-energy parameters L_i appear, together with additional ones (W_i) describing lattice artifacts.

The mixed mesons, whose masses $m_{\rm VS}$ we have also calculated, become degenerate with the pions in the special case $m_{\rm V} = m_{\rm S}$. In this case the expression reduces to

$$\begin{aligned} m^2_\pi = {} & \chi + \rho + \frac{(\chi+\rho)^2}{16\pi^2 F_0^2}\ln\left(\frac{\chi+\rho}{16\pi^2 F_0^2}\right) \\ & + \frac{8}{F_0^2}\Big[(2L_8 - L_5 + 2L_6 - L_4)\chi^2 \\ & + (2W_8 + 2W_6 - W_5 - W_4 - L_5 - L_4)\chi\rho\Big] . \end{aligned} \tag{16}$$

To leading order the PCAC quark mass obeys $2B_0 m^{\rm R}_{\rm PCAC} = \chi + \rho$, and we recognize the Gell-Mann–Oakes–Renner relation

$$m^2_\pi = 2B_0 m^{\rm R}_{\rm PCAC} + \mathrm{NLO} \,. \tag{17}$$

Including terms in next-to-leading (NLO) order, we can express m^2_π in terms of $m^{\rm R}_{\rm PCAC}$ as

$$\begin{aligned} m^2_\pi = {} & \chi_{\rm PCAC} + \frac{\chi^2_{\rm PCAC}}{16\pi^2 F_0^2}\ln\frac{\chi_{\rm PCAC}}{\Lambda^2} \\ & + \frac{8}{F_0^2}\left[(2L_8 - L_5 + 2L_6 - L_4)\chi^2_{\rm PCAC}\right. \\ & + (W_8 + W_6 - W_5 - W_4 \\ & \left. - 2L_8 + L_5 - 2L_6 + L_4)\chi_{\rm PCAC}\rho\right] , \end{aligned} \tag{18}$$

where we define

$$\chi_{\rm PCAC} = 2B_0 m^{\rm R}_{\rm PCAC} \,. \tag{19}$$

As a remark, in the case $m_{\rm V} = m_{\rm S}$ the masses can alternatively be obtained from the partially quenched theory

with symmetry SU(2|1) by considering mixed pions made from a valence quark and a degenerate sea quark. Indeed, calculating the masses in this model reproduces (16).

The η_s can be included in the analysis by relaxing the constraint of a vanishing supertrace [37, 45], and associating it with the field

$$\Phi_0(x) = \mathrm{sTr}\Phi(x). \tag{20}$$

The effective Lagrangian then contains additional terms depending on Φ_0:

$$\Delta\mathcal{L} = \alpha\partial_\mu\Phi_0\partial_\mu\Phi_0 + m_\Phi^2\Phi_0^2 + \mathcal{O}\left(\Phi_0^3\right) , \tag{21}$$

where α and m_Φ are free parameters in this context. We content ourselves with displaying only the leading-order expression for the mass of the η_s, which reads

$$m_{\eta_s}^2 = \frac{m_\Phi^2 + \chi_{\mathrm{PCAC}}}{1+\alpha}. \tag{22}$$

Our numerical results for m_{η_s} allow us to determine α and m_Φ.

4 Numerical simulations

After some preparatory search in the parameter space we concentrated our runs on the $12^3 \cdot 24$ lattice to $\beta = 3.8$ and those on $16^3 \cdot 32$ to $\beta = 4.0$. The parameter values, the number of analysed configurations, the average plaquette, its integrated autocorrelation and the value of the Sommer scale parameter in lattice units r_0/a are summarised in Table 2. As one can see, taking the values of r_0/a at the highest κ (smallest quark masses), the extensions of the 12^3 and 16^3 lattices are $L = 4.46\, r_0 = 2.23$ fm and $L = 4.29\, r_0 = 2.14$ fm, respectively. Since we fix $r_0 = 0.5$ fm by definition, these correspond to lattice spacings $a = 0.186$ fm and $a = 0.134$ fm, respectively.

In the update chain by the PHMC algorithm with stochastic correction [27, 28] a *sequence of PHMC trajectories* is followed by a Metropolis accept–reject step with a higher precision polynomial. The total length of the trajectory sequence in the runs in Table 2 was between 1.5 and 1.8. The sequences consisted out of 3–6 individual trajectories. The precision of the first step of polynomial approximations was tuned such that the acceptance of the PHMC trajectories was about 0.80–0.85. The total length of the trajectory sequence was chosen such that the acceptance of the Metropolis test was again 0.80–0.85. This ensured a relatively high total acceptance of 0.64–0.72. During the runs we tried to optimise the parameters of PHMC. The different values of the *integrated autocorrelation times* for the average plaquette in Table 2 are, in fact, mainly due to increasingly better optimisations and not so much to the dependence on the run parameters.

Table 2. Summary of the runs: $12^3 \cdot 24$ and $16^3 \cdot 32$ lattices have lowercase and uppercase labels, respectively. The number of gauge configurations, which were saved after every trajectory sequence, is N_{conf}. The average plaquette value, its autocorrelation in number of trajectory sequences τ_{plaq} and the value of r_0/a are also given

label	β	κ	N_{conf}	plaquette	τ_{plaq}	r_0/a
a	3.80	0.1700	5424	0.546041(66)	12.5	2.66(4)
b	3.80	0.1705	3403	0.546881(46)	4.6	2.67(5)
c	3.80	0.1710	2884	0.547840(67)	7.6	2.69(5)
A	4.00	0.1600	1201	0.581427(36)	4.3	3.56(5)
B	4.00	0.1610	1035	0.582273(36)	4.1	3.61(5)
C	4.00	0.1615	1005	0.582781(32)	3.3	3.73(5)

The second step approximations were more than good enough to ensure that the expectation values were completely unaffected by the remaining small imprecision. (See, for instance, the small relative deviations in Table 1.) This has also been explicitly checked by performing a final stochastic correction on a large sample of configurations with polynomials P' of order 2500 in the stochastic part of the right hand side of (6).

For the calculation of the expectation values the reweighting procedure according to (8) has to be carried out. For this, besides the correction factor $C[U]$ from (7), also the sign of the fermion determinant $\sigma[U]$ is needed. This we calculated by the *spectral flow* method [34]. For the κ-dependent computation of the low-lying eigenvalues of the hermitean fermion matrix $Q[U]$ we followed [35].

It turned out that the effect of the correction factors $\sigma[U]C[U]$ is in most cases negligible. For instance, in run b of Table 2 the average value of $\sigma[U]C[U]$ in the denominator is 0.9982. In run c it is 0.9842. In run b there are 34 configurations out of 3403, where some eigenvalue is outside the approximation interval $[\epsilon, \lambda]$ and out of them there is a single one with negative fermion determinant. In run c there are 167 from 2884 outside $[\epsilon, \lambda]$ and out of them there are 26 with negative correction factor due to $\sigma = -1$.

Since the sign of the fermion determinant was not determined on every configuration, the question arises whether perhaps some negative signs were missed. This is very improbable, because we determined the sign also on the neighbouring configurations in addition to those with small eigenvalues and out of the remaining configurations we have chosen 100 randomly for sign determination. None of these additional configurations turned out to have a negative determinant.

In the average plaquette and r_0/a the effect of the correction factors is completely negligible. For instance, in runs b and c the correction has an effect in the average value of r_0/a only in the fifth digit – whereas the statistical error is in the third digit. In all other runs besides b and c every eigenvalue is inside the approximation interval $[\epsilon, \lambda]$ and therefore, according to (7), the correction factor is equal to 1 on every configuration.

4.1 Results for hadron masses

Starting with the mesonic states, we consider the simplest interpolating operators in the pseudoscalar and scalar

sectors:

$$0^+: \quad P(x) = \bar{\psi}(x)\gamma_5\psi(x)\,, \tag{23}$$

$$0^-: \quad S(x) = \bar{\psi}(x)\psi(x)\,. \tag{24}$$

We denote by η_s and σ_s the corresponding hadron states at the lowest end of the energy spectrum (the usual notation J^P is used for the respective quantum numbers). The corresponding states in the QCD spectrum with the same quantum numbers are $\eta'(958)$ and $f_0(600)$ (or σ). (Note, however, that the states in QCD are linear combinations of $\bar{u}u$, $\bar{d}d$ and $\bar{s}s$ components – in contrast to the states in $N_f = 1$ QCD which are built out of a single quark flavour.)

In the case of the pseudoscalar mesons, invariance under the flavour group plays a special role when comparing with QCD states because of the U(1) axial anomaly. (This is not the case for baryons; see the following.)

Analogously to flavour singlet mesons in QCD, the correlators of the above interpolating operators contain disconnected diagrams. These were computed by applying stochastic estimator techniques (SET), and in particular the variant of [46] with Z_2 noise and spin dilution. The method was already applied to the case of SYM [47] (as mentioned in the introduction, SYM shares many similarities with $N_f = 1$ QCD). In order to optimise the computational load, taking also autocorrelations into account, every fifth configuration was typically analysed, with 20 stochastic estimates each.

Spin 0 states can also be build by purely gluonic operators. These are well known objects of investigation in lattice QCD were they should describe the glueballs. Due to the expected signal–noise ratio of their purely gluonic correlation they belong to the most notorious particles to measure. In particular the 0^{++} glueball has the same quantum numbers as the σ_s meson. As a consequence, these two states can also mix with each other but in this first investigation we neglect the mixing and consider only diagonal correlators for both states.

We used the single spatial plaquette to obtain the mass of the 0^{++} ground state. To increase the overlap of the operator with this state we used APE smearing and also performed variational methods to obtain optimal glueball operators from linear combinations of the basic operators.

We now come to the baryon sector. The simplest baryonic interpolating field which can be built out of one quark flavour is

$$\Delta_i(x) = \epsilon_{abc}\left[\psi_a(x)^{\mathrm{T}} C\gamma_i\psi_b(x)\right]\psi_c(x)\,. \tag{25}$$

The above operator also contains a spin 1/2 component, implying that the spin 3/2 component, on which we focus, must be projected out from the spinorial correlator,

$$G_{ji}(t) = \sum_{\mathbf{x}} \left\langle \Delta_j(\mathbf{x},t)\bar{\Delta}_i(0)\right\rangle\,. \tag{26}$$

We follow [48] and consider the spin-projected correlator

$$G_{3/2}(t) = \frac{1}{6}\mathrm{Tr}\left[G_{ji}(t)\gamma_j\gamma_i + G_{ii}(t)\right]\,. \tag{27}$$

The low-lying hadron state contributing to the above correlator is expected to have positive parity ($\frac{3}{2}^+$). This corresponds to the $\Delta(1232)^{++}$ of QCD if our dynamical fermion is interpreted as an u quark. If the dynamical fermion is taken to be the s quark then this would be the Ω^- baryon. (However, spin and parity of the corresponding particle have not yet been measured, so the identification of this state with the Ω^- baryon is still uncertain [49].) In correspondence to η_s and σ_s, in what follows we call this state Δ_s. (Here one can interpret the index s as referring to the "sea" quark.)

It should be noted at this point that the above QCD states are not flavour singlets in $N_f = 3$ QCD (and in the one flavour partially quenched theory). We recall here that interpolating fields corresponding to flavour singlet baryon states cannot be build in QCD if only quark fields are considered as ingredients.

The results of the hadron masses are reported in Table 3 and, as a function of the bare PCAC quark mass m_{PCAC}, in Fig. 1. In the figure the masses are multiplied by the Sommer scale parameter r_0; therefore, one can put the results for both lattice spacings in a single plot and check their scaling. (The expected small change of the multiplica-

Table 3. Results for light hadron masses in $N_f = 1$ QCD

run	am_{η_s}	am_{σ_s}	$am_{0^{++}}$	am_{Δ_s}
a	0.462(13)	0.660(39)	0.777(11)	1.215(20)
b	0.403(11)	0.629(29)	0.685(10)	1.116(38)
c	0.398(28)	0.584(55)	0.842(16)	1.204(57)
A	0.455(17)	0.607(57)	1.083(79)	1.006(15)
B	0.380(18)	0.554(52)	1.032(66)	0.960(15)
C	0.316(22)	0.613(67)	0.980(97)	0.876(26)

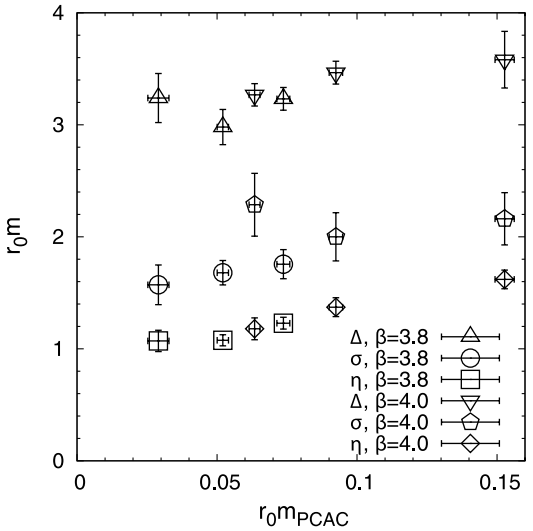

Fig. 1. The mass of the lightest physical particles in one-flavour QCD as a function of the PCAC quark mass. The masses are multiplied by the scale parameter r_0 in order to obtain dimensionless quantities

tive renormalisation factor of $m_{\rm PCAC}$ between $\beta = 3.8$ and $\beta = 4.0$ is neglected here.)

Only in the case of run c the measurement correction has a sizeable effect on the mass estimates. In this case configurations with negative determinant where singled out: the sign of the determinant has the effect of pushing the masses up by 7%–10%.

The errors on the glueball mass are rather large – especially on the $16^3 \cdot 32$ lattice at $\beta = 4.0$ – therefore, they are not shown in the figure. Obviously, our statistics is not sufficient for this purpose. In general a larger number of configurations would improve the determinations in the glueball sector. Since the computational load is in this case negligible, for future runs we plan a more frequent storage of the gauge configuration.

4.1.1 Valence analysis

The connected contribution to the meson correlators can be interpreted as a non-singlet meson made up of valence quarks in the partially quenched picture; see Sect. 3. The pseudoscalar channel corresponds in particular to the "valence" pion. Since the computation of the connected diagrams is less demanding, we could afford the analysis of the complete set of configurations.

In the baryon sector, one can define a "valence" nucleon, with the usual projector operator

$$N(x) = \epsilon_{abc}[\psi_a(x)^{\rm T} C \psi'_b(x)]\psi_c(x)\,, \tag{28}$$

where ψ' can be interpreted as the field of the valence quark.

The results concerning valence hadron masses are reported in Table 4 and Fig. 2. In addition, the bare PCAC quark mass according to the definition in (10) and the bare pion decay constant in lattice units af_π are also included. f_π and its renormalised counterpart $f_\pi^{\rm R}$ are defined as

$$\begin{aligned} af_\pi &= (am_\pi)^{-1}\langle 0|A^+_{x=0,\mu=0}|\pi^-(\mathbf{p}=0)\rangle\,, \\ f_\pi^{\rm R} &= Z_{\rm A} f_\pi\,, \end{aligned} \tag{29}$$

where $A^+_{x\mu}$ is the axialvector current as in (10) and $\pi^-(\mathbf{p}=0)$ is a pion state with zero momentum. (The normalisation of f_π is such that in nature we have $f_\pi^{\rm R} \simeq 130\,{\rm MeV}$.) The value of af_π on the lattice is obtained by the method described in [50]. In Fig. 2 the masses are multiplied by the scale parameter r_0 in order to obtain dimensionless variables.

Table 4. The PCAC quark mass $m_{\rm PCAC}$, the pion mass m_π and decay constant f_π, and the nucleon mass m_N in lattice units

run	$am_{\rm PCAC}$	am_π	af_π	$am_{\rm N}$
a	0.02771(45)	0.3908(24)	0.1838(11)	1.0439(54)
b	0.01951(39)	0.3292(25)	0.1730(15)	0.956(27)
c	0.0108(12)	0.253(10)	0.156(10)	1.011(51)
A	0.04290(36)	0.4132(21)	0.1449(9)	0.9018(44)
B	0.02561(31)	0.3199(22)	0.1289(10)	0.7978(53)
C	0.01700(30)	0.2635(24)	0.1188(12)	0.734(10)

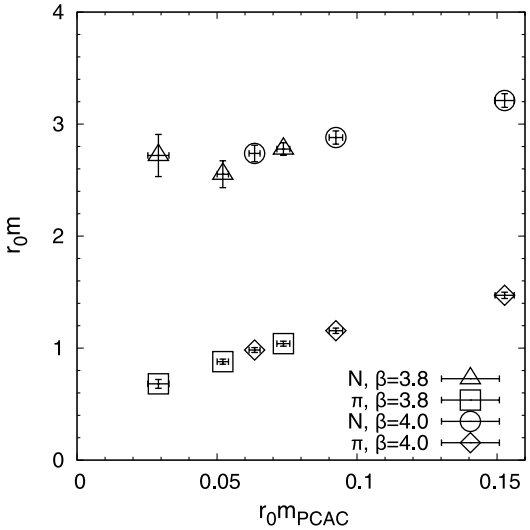

Fig. 2. The mass of the valence pion and nucleon as a function of the bare PCAC quark mass

4.1.2 Chiral perturbation theory fits

The properties of the valence pion (pion mass m_π and decay constant $f_\pi^{\rm R}$) can be analysed in partially quenched ChPT. We fit $a^2m_\pi^2$ and af_π simultaneously as a function of $am_{\rm PCAC}$ including the data at both values of β. There are not enough data to account for the lattice artifacts. Therefore the fit is done with the continuum formulae

$$\begin{aligned} m_\pi^2 &= \chi_{\rm PCAC} + \frac{\chi^2_{\rm PCAC}}{16\pi^2 F_0^2}\ln\frac{\chi_{\rm PCAC}}{\Lambda_3^2}\,, \\ \frac{f_\pi^{\rm R}}{F_0\sqrt{2}} &= 1 - \frac{\chi_{\rm PCAC}}{32\pi^2 F_0^2}\ln\frac{\chi_{\rm PCAC}}{\Lambda_4^2}\,, \end{aligned} \tag{30}$$

with the low-energy constants

$$\begin{aligned} \Lambda_3 &= 4\pi F_0 \exp\{64\pi^2(L_4+L_5-2L_6-2L_8)\}\,, \\ \Lambda_4 &= 4\pi F_0 \exp\{64\pi^2(L_4+L_5)\}\,. \end{aligned} \tag{31}$$

The changes of the renormalisation constants $Z_{\rm A}$ and $Z_{\rm P}$ between the two β values are neglected. The results are displayed in Figs. 3 and 4.

Owing to the fact that the number of degrees of freedom in the fit is small, the uncertainty of the fit parameters is relatively large. The determination of the universal low-energy scales Λ_3/F_0 and Λ_4/F_0 can be improved by considering the ratios [16, 17, 55]

$$\frac{m_\pi^2}{m_{\pi,{\rm ref}}^2}\,, \quad \frac{f_\pi}{f_{\pi,{\rm ref}}}\,, \tag{32}$$

in which some of the coefficients cancel. We consider the data on the larger lattice at $\beta = 4.0$ and take the quantities

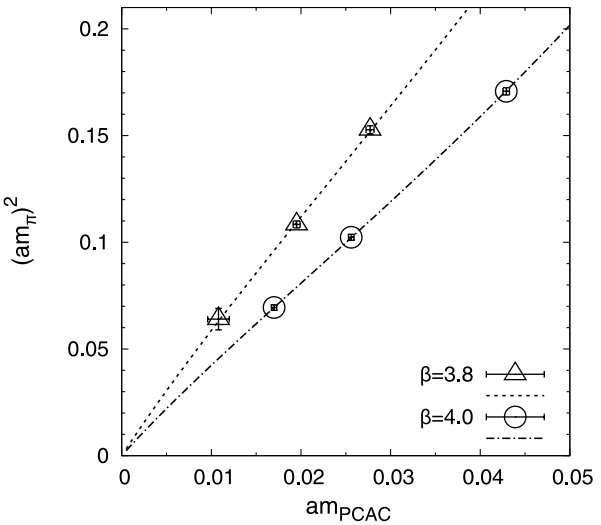

Fig. 3. Pion masses squared in lattice units and the results of the PQChPT fit

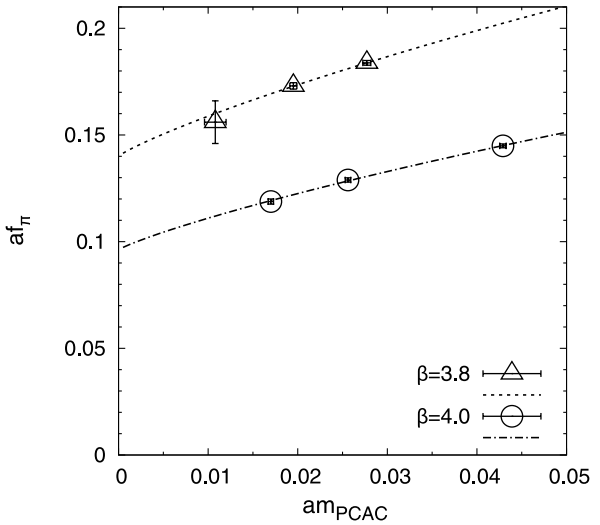

Fig. 4. Pion decay constants in lattice units and the results of the PQChPT fit

at $\kappa = 0.1615$ as reference. The fit yields

$$\frac{\Lambda_3}{F_0} = 10.0 \pm 2.6\,, \tag{33}$$

$$\frac{\Lambda_4}{F_0} = 31.5 \pm 14.3\,, \tag{34}$$

which is compatible with the phenomenological values from ordinary QCD [51, 52].

In order to estimate the parameters α and m_Φ, related to the mass of the η_s (see Sect. 3), we made a fit of m_π^2 and $m_{\eta_s}^2$ at $\beta = 4.0$ in leading-order ChPT. The result is

$$\alpha = -0.03(19)\,, \quad am_\Phi = 0.18(8)\,, \tag{35}$$

indicating the vanishing of α. Fixing $\alpha = 0$ in the fit yields

$$am_\Phi = 0.19(2) \quad \text{or} \quad r_0 m_\Phi = 0.72(10)\,, \tag{36}$$

where the value of r_0/a extrapolated to vanishing PCAC quark mass is used.

This constant, whose value in physical units is $m_\Phi = 284(40)$MeV, can be related to the quenched topological susceptibility $\chi_{\rm t}$ through the Witten–Veneziano formula [53, 54]

$$m_\Phi^2 = \frac{4N_f}{(f_\pi^{\rm R})^2}\chi_{\rm t}\,, \tag{37}$$

which is valid in leading order of the $1/N_c$ expansion. With $\chi_{\rm t} = (193 \pm 9\ {\rm MeV})^4$ [56] and our value for f_π^R we would obtain $m_\Phi = 426$ MeV.

5 Discussion

This first Monte Carlo investigation of the hadron masses in QCD with $N_f = 1$ dynamical quark flavour reveals the qualitative features of the low-lying particle spectrum in this theory. The spatial extensions of our $12^3 \cdot 24$ and $16^3 \cdot 32$ lattices are about $L \simeq 2.2$ fm (see Table 2).[1] This implies lattice spacings $a \simeq 0.19$ fm and $a \simeq 0.13$ fm, respectively. The (bare) quark masses are reasonably small – in a range 10–30 MeV and 25–60 MeV on the $12^3 \cdot 24$ and $16^3 \cdot 32$ lattice, respectively. The updating algorithm we use (PHMC with stochastic correction [27, 28]) works fine in this range, making the extension of the Monte Carlo investigations towards larger volumes, smaller quark masses and smaller lattice spacings straightforward. In the present runs the fluctuation of the eigenvalues of the fermion matrix towards exceptionally small (or negative) values can be easily handled by reweighting the configurations during the evaluation of the expectation values. In fact, except for the run with the smallest quark mass on the $12^3 \cdot 24$ lattice where the reweighting has a small effect, the reweighting is completely negligible or even unnecessary.

The lightest hadron is the pseudoscalar meson bound state of a quark and an antiquark – the η_s meson (see Table 3 and Fig. 1). The corresponding scalar bound state – the σ_s meson – is in our points by about a factor 1.5 heavier. Compared to the estimate in [13, 14] $m_{\sigma_s}/m_{\eta_s} \simeq N_c/(N_c - 2) = 3$ this result is too low, but the situation could be better in the zero quark mass limit that the prediction of [13, 14] applies to. The lightest baryon – the Δ_s baryon – is by a factor of about 3 heavier than the η_s meson. The lightest glueball lies between the σ_s meson and the Δ_s baryon, but its mass could not be properly measured on the $16^3 \cdot 32$ lattice with our statistics. In general, the mass measurements have relatively large errors – between 3%–10% – and no infinite volume and continuum limit extrapolations could be performed with our present data. We hope to return to these questions and to give more precise results in future publications.

An interesting aspect of $N_f = 1$ QCD is the possibility of a *partially quenched* extension with valence quarks. In

[1] In order to have some relation to the scales in real QCD, we set the Sommer scale parameter by definition to be $r_0 \equiv 0.5$ fm.

particular, adding two valence quarks, the model has similarities to QCD in nature with its three light (u, d and s) quark flavours. A theoretically interesting special case is if all three quarks, the dynamical one and the two valence ones, have exactly equal masses. In this case there is an exact SU(3) flavour symmetry. This can be exploited for the introduction of a quark mass by defining it as the PCAC quark mass in the partially quenched theory. In this extended model there exist the usual light hadron states well known from real QCD: the pseudoscalar pseudo-Goldstone bosons (pions etc.), the nucleon etc. The results for the masses of the lightest states and the decay constant of the pseudoscalar bosons are collected in Table 4 and also shown in Fig. 2.

Since the physical volumes of the 12^3 and 16^3 lattices are to a good approximation equal, the comparison of the results at the two different lattice spacings gives a hint for the magnitude of the deviations from the continuum limit. As one can see in Figs. 1 and 2, the scaling between $\beta = 3.8$ and $\beta = 4.0$ is reasonably good – especially for the lightest states η_s and π. However, for reliable continuum limit estimates more data at several lattice spacings are required.

In the pseudoscalar sector of the partially quenched model one can apply partially quenched chiral perturbation theory for fitting the mass and the decay constant. As Figs. 3 and 4 show, the NLO formulae give good fits but the number of degrees of freedom in the fits is small, and therefore the uncertainty of the fit parameters is relatively large.

Acknowledgements. We are grateful to Luigi Scorzato for valuable discussions and for helping us in the set-up of the programs for investigating the eigenvalue spectrum of the fermion matrix. We thank the computer centers at DESY Hamburg and NIC at Forschungszentrum Jülich for providing us the necessary technical help and computer resources. This work is supported in part by the Deutsche Forschungsgemeinschaft under grant Mu757/13-1. E.S. is supported by the U.S. Dept. of Energy under contract DE-AC02-98CH10886.

References

1. R.F. Dashen, Phys. Rev. D **3**, 1879 (1971)
2. C. Vafa, E. Witten, Nucl. Phys. B **234**, 173 (1984)
3. M. Creutz, Rev. Mod. Phys. **73**, 119 (2001) [hep-lat/0007032]
4. M. Creutz, hep-lat/0511052
5. M. Creutz, Phys. Rev. Lett. **92**, 201601 (2004) [hep-lat/0312018]
6. M. Creutz, Ann. Phys. **322**, 1518 (2007) [hep-th/0609187]
7. A. Armoni, M. Shifman, G. Veneziano, Nucl. Phys. B **667**, 170 (2003) [hep-th/0302163]
8. A. Armoni, M. Shifman, G. Veneziano, Phys. Rev. Lett. **91**, 191601 (2003) [hep-th/0307097]
9. A. Armoni, M. Shifman, G. Veneziano, Phys. Lett. B **579**, 384 (2004) [hep-th/0309013]
10. A. Armoni, M. Shifman, G. Veneziano, hep-th/0403071
11. P. Keith-Hynes, H.B. Thacker, Phys. Rev. D **75**, 085001 (2007) [hep-th/0701136]
12. G. Veneziano, S. Yankielowicz, Phys. Lett. B **113**, 231 (1982)
13. F. Sannino, M. Shifman, Phys. Rev. D **69**, 125004 (2004) [hep-th/0309252]
14. A. Armoni, E. Imeroni, Phys. Lett. B **631**, 192 (2005) [hep-th/0508107]
15. T. DeGrand, R. Hoffmann, S. Schaefer, Z. Liu, Phys. Rev. D **74**, 054501 (2006) [hep-th/0605147]
16. qq+q Collaboration, F. Farchioni, I. Montvay, E. Scholz, L. Scorzato, Eur. Phys. J. C **31**, 227 (2003) [hep-lat/0307002]
17. qq+q Collaboration, F. Farchioni, I. Montvay, E. Scholz, Eur. Phys. J. C **37**, 197 (2004) [hep-lat/0403014]
18. L. Del Debbio, L. Giusti, M. Lüscher, R. Petronzio, N. Tantalo, JHEP **0602**, 011 (2006) [hep-lat/0512021]
19. M. Göckeler et al., PoS **LAT2006**, 179 (2006) [hep-lat/0610066]
20. ETM Collaboration, P. Boucaud et al., Phys. Lett. B **650**, 304 (2007) [hep-lat/0701012]
21. R. Sommer, Nucl. Phys. B **411**, 839 (1994) [hep-lat/9310022]
22. C. Alexandrou, A. Borici, A. Feo, P. de Forcrand, A. Galli, F. Jegerlehner, T. Takaishi, Phys. Rev. D **60**, 034504 (1999) [hep-lat/9811028]
23. K. Symanzik, Nucl. Phys. B **226**, 187 (1983)
24. P. Weisz, Nucl. Phys. B **212**, 1 (1983)
25. P. Weisz, R. Wohlert, Nucl. Phys. B **236**, 397 (1984)
26. P. Weisz, R. Wohlert, Nucl. Phys. B **247**, 544 (1984)
27. I. Montvay, E. Scholz, Phys. Lett. B **623**, 73 (2005) [hep-lat/0506006]
28. E.E. Scholz, I. Montvay, PoS **LAT2006**, 037 (2006) [hep-lat/0609042]
29. R. Frezzotti, K. Jansen, Phys. Lett. B **402**, 328 (1997) [hep-lat/9702016]
30. R. Frezzotti, K. Jansen, Nucl. Phys. B **555**, 395 (1999) [hep-lat/9808011]
31. R. Frezzotti, K. Jansen, Nucl. Phys. B **555**, 432 (1999) [hep-lat/9808038]
32. P. de Forcrand, T. Takaishi, Nucl. Phys. Proc. Suppl. **53**, 968 (1997) [hep-lat/9608093]
33. I. Montvay, Nucl. Phys. B **466**, 259 (1996) [hep-lat/9510042]
34. R.G. Edwards, U.M. Heller, R. Narayanan, Nucl. Phys. B **535**, 403 (1998) [hep-lat/9802016]
35. T. Kalkreuter, H. Simma, Comput. Phys. Commun. **93**, 33 (1996) [hep-lat/9507023]
36. A. Morel, J. Phys. (Paris) **48**, 1111 (1987)
37. C.W. Bernard, M.F.L. Golterman, Phys. Rev. D **49**, 486 (1994) [hep-lat/9306005]
38. S.R. Sharpe, Phys. Rev. D **56**, 7052 (1997)
39. S.R. Sharpe, Phys. Rev. D **62**, 099901 (2000) [hep-lat/9707018]
40. S.R. Sharpe, R.L. Singleton, Phys. Rev. D **58**, 074501 (1998) [hep-lat/9804028]
41. W.J. Lee, S.R. Sharpe, Nucl. Phys. Proc. Suppl. **73**, 240 (1999) [hep-lat/9809026]
42. G. Rupak, N. Shoresh, Phys. Rev. D **66**, 054503 (2002) [hep-lat/0201019]
43. S. Aoki, Phys. Rev. D **68**, 054508 (2003) [hep-lat/0306027]
44. O. Bär, G. Rupak, N. Shoresh, Phys. Rev. D **70**, 034508 (2004) [hep-lat/0306021]
45. S.R. Sharpe, N. Shoresh, Phys. Rev. D **64**, 114510 (2001) [hep-lat/0108003]
46. TXL Collaboration, J. Viehoff et al., Nucl. Phys. Proc. Suppl. **63**, 269 (1998) [hep-lat/9710050]

47. F. Farchioni, R. Peetz, Eur. Phys. J. C **39**, 87 (2005) [hep-lat/0407036]
48. A.M. Abdel-Rehim, R. Lewis, R.M. Woloshyn, Phys. Rev. D **71**, 094 505 (2005) [hep-lat/0503007]
49. Particle Data Group, W.M. Yao et al., J. Phys. G **33**, 1 (2006)
50. F. Farchioni, C. Gebert, I. Montvay, L. Scorzato, Eur. Phys. J. C **26**, 237 (2002) [hep-lat/0206008]
51. J. Gasser, H. Leutwyler, Ann. Phys. **158**, 142 (1984)
52. S. Dürr, Eur. Phys. J. C **29**, 383 (2003) [hep-lat/0208051]
53. E. Witten, Nucl. Phys. B **156**, 269 (1979)
54. G. Veneziano, Nucl. Phys. B **159**, 213 (1979)
55. ALPHA Collaboration, J. Heitger, R. Sommer, H. Wittig, Nucl. Phys. B **588**, 377 (2000) [hep-lat/0006026]
56. S. Dürr, Z. Fodor, C. Hoelbling, T. Kurth, JHEP **0704**, 055 (2007) [hep-lat/0612021]